

Wettability of mineral and metallic powders: applicability and limitations of sessile drop method and Washburn's technique

Laura Susana^a, Filippo Campaci^b, Andrea C. Santomaso^{a,*}

^a *DII – Department of Industrial Engineering, University of Padova
Via Marzolo 9, 35131, Padova, Italy*

^b *Fileur® - Trafilerie di Cittadella, Via Mazzini 69, 35013, Cittadella, Italy*

Corresponding author: Andrea Santomaso; email: andrea.santomaso@unipd.it

Keywords: Wettability; Contact angle; Minerals powders; Washburn's method

Abstract

Characterization of powder wettability is a prerequisite to the understanding of many processes of industrial relevance such as agglomeration which spans from pharmaceutical and food applications to metallurgical ones. The choice of the wetting fluid is crucial: liquid must wet the powder in order for agglomeration to be successful. Different methods for wettability assessment of powders were reported in the literature, however the sessile drop method and capillary rise test remain among the most widely employed because they are easy to perform and inexpensive. In this paper, the application and limitations of sessile drop method and capillary rise test on mineral and metallic surface were discussed. This work provides a collection of wettability measurements using several powders and liquid binders which are involved in the manufacturing process of welding wires. Moreover a new reference liquid for the calibration of capillary rise method was proposed.

1. Introduction

Wet granulation of fine powders is carried out in many industries, from pharmaceutical and agrochemical industries to mineral and metallurgical ones, to improve physical and material properties of powders such as flowability, rate of dissolution and robustness to segregation [1–3]. Knowledge of wetting attitude of the liquid binder through the feed powder is therefore a prerequisite for understanding and controlling any wet granulation process since the binder is used to form liquid bridges between the solid particles [4]. Experimental method for wettability assessment of powders have been recently reviewed [5-6]. Wettability describes the ability of a surface to be wetted by the probing liquid and it can be characterized by different parameters. The wettability of solid surface is generally characterized in terms of the contact angle, θ , i.e. the angle between the tangent to powder bed surface and the tangent to the liquid drop at the vapour-liquid-solid intersection [7]. The contact angle is a useful and concise indicator of hydrophobic characteristics of solids.

When a small drop of liquid is placed on solid substrate, it assumes a shape that minimizes the free energy of the system. Young's equation represents the equilibrium conditions between three interfacial tensions, the solid–vapour γ_{SV} , solid–liquid γ_{SL} and liquid–vapour γ_{LV} :

$$\gamma_{LV} \cos \theta = \gamma_{SV} - \gamma_{SL} \quad (1)$$

Eq. (1) implies the existence of one equilibrium contact angle and it is valid for ideal solid surface, which means a homogeneous and flat surface. The contact angle approach is conceptually easy to apply for a flat, smooth and chemically homogeneous surface. Unfortunately real surfaces depart from this assumption because of surface roughness and chemical heterogeneity. Furthermore wettability of finely divided solids depends on variables such as particle size and porosity of the powder bed beside the molecular interactions between the phases entering into contact [8]. Due to surface irregularities, molecular orientation and partial dissolution of the solid in the fluid, the contact angle may change along the contact line from one point to another. Three distinct contact angle can be assumed to exist: the intrinsic, the apparent and the actual one [9].

For an ideal surface the contact angle does not change along the contact line and it is called *intrinsic* contact angle (Figure 1a). The *actual* contact angle on a real surface is instead the angle between the tangent to the surface at a given point and the tangent to the liquid droplet in the same point (Figure 1b). Finally the *apparent* contact angle is measured between the tangent to the liquid surface and the tangent to the powder surface assumed as if it was ideal (Figure 1c). Moreover it is known that a range of stable apparent angles, referred to as hysteresis, can be measured on a real surface depending on the conditions in which angles are measured (advancing or receding) [6]. Figure 1 illustrates the three different definitions of the contact angles.

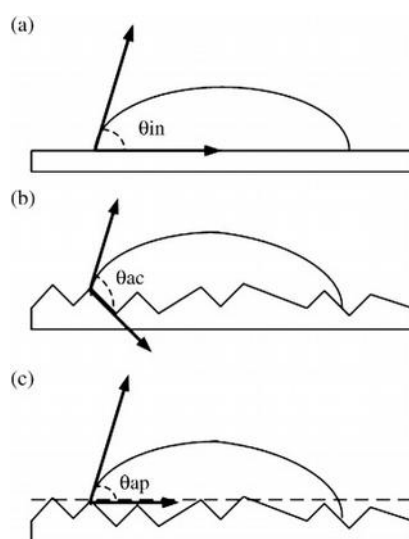


Fig. 1. Definition of the contact angles: (a) the intrinsic contact angle, (b) the actual contact angle and (c) the apparent contact angle.

In order to characterize the wetting behavior of porous media such as powder systems, experimental methods require to form tablets or compacts by exerting a pressure before conducting contact angle measurements. In this case, imbibition of a single droplet into a porous media depends on powder bed porosity and the size and orientation of the pores. Kossen and Heertjes [10] developed a method to relate the actual contact angle, θ , to the apparent contact angle, θ' and powder porosity, ε :

$$(1 - \varepsilon) \cos \theta = \cos \theta' - \varepsilon \quad (2)$$

In general, methods for wettability assessment of finely divided solids can be divided into two categories: methods based on direct observation of the solid/liquid interface such as the sessile drop method [10], the flotation technique [11] and on the other hand techniques based on wetting processes (adhesive, spreading, condensation and immersional wetting) such as the capillary rise test known also as Washburn test [12], the equilibrium height method [13] and inverse gas chromatography [14]. The first category of method can be used if powder is homogeneous and for small particles (smaller than 500 μm) and they provide the apparent contact angle measurement by the direct analysis of drop shape [5]. The other techniques are indirect measure of the apparent contact angle: for instance in Washburn method the contact angle between the liquid and the capillary surface is evaluated by measuring the liquid rising speed.

Most of the reports in the literature have focused on wetting and agglomeration phenomena concerning pharmaceutical powders like lactose and salicylic acid powders with water and PVP and PEG solutions [15-19]. A few studies deal with the capillary rise experiments on silica flour, calcium carbonate and glass [20-22]. Nonetheless, less attention has been paid so far to the wettability of mineral and metallic powders [23] even though they are involved in many important processes such as the manufacture of ceramics, welding wires, rods and electrodes and powder metallurgy. The goal of our study was to examine use and limit of Washburn technique and of sessile drop method for mineral and metallic solids (mainly involved in the welding wire production through a granulation process) and in particular to find an appropriate reference liquid for Washburn calibration method.

2. Theory

In a typical Washburn test, a cylindrical tube with a permeable filter at the bottom is filled with the powder sample. The bottom of the tube is brought into contact with the wetting liquid so that the fluid can rise into the tube because of capillary forces and the liquid front rising in the vertical tube is observed. An equation that describes the penetration of a liquid into a cylindrical capillary is the Hagen–Poiseuille's law:

$$v = \frac{dh}{dt} = \frac{r_c^2}{8\mu h} \Delta P, \quad (3)$$

where v is the liquid rising speed, h denotes the distance penetrated by the liquid, t is the time of infiltration, r_c is the radius of the capillary, η is viscosity of the probing liquid and ΔP is the pressure difference across the invading liquid meniscus.

The driving pressure is given by the sum of a capillary pressure described by Laplace equation and a hydrostatic pressure:

$$\Delta P = \frac{2\gamma_{LV} \cos \theta}{r_c} + \rho gh \quad (4)$$

g is the gravitational force, ρ is the liquid density and γ_{LV} is the liquid–air interfacial tension. If the liquid weight can be neglected, integration of Eq. (3) for the boundary condition $h = 0$ when $t = 0$ leads to the well-know Washburn's equation for one capillary:

$$\frac{h^2}{t} = \frac{r_C \gamma_{LV} \cos \theta}{2\eta} \quad (5)$$

According to this model, a bed of powder can be modelled as an array of parallel capillaries with constant radius where penetration into the substrate is driven just by capillarity and the following conditions are applied: (i) steady-state laminar flow, (ii) no slip of the fluid along the porous wall, (iii) no externally applied pressure. Under these conditions and with a Newtonian fluid the Washburn's equation predicts that a plot of h^2 vs. t is a straight line.

Using the Kozeny approach the radius r_C is replaced by the equivalent or effective radius, r_{eff} which accounts for the non-ideality of the system, particularly the porosity and tortuosity of a granular substrate. The equivalent radius is defined as:

$$r_{eff} = 2R_h \quad (6)$$

where R_h is the hydraulic radius defined as the ratio between the cross section available for flow and the wetted perimeter. In terms of unit volume of powder bed the hydraulic radius can be expressed as:

$$R_h = \frac{\varepsilon}{a} = \frac{\varepsilon}{a_s(1-\varepsilon)} \quad (7)$$

where ε is the bed porosity, a is the ratio of the wetted surface and the bed volume and a_s is the particle specific surface area which for spherical particle is $6/d_{32}$. In order to account for non-sphericity of the particles a shape factor ϕ is also introduced and Eq. (7) becomes:

$$R_h = \frac{d_{32} \varepsilon \phi}{6(1-\varepsilon)} \quad (8)$$

where d_{32} is the Sauter's mean diameter of the particles.

In this work Washburn's equation was expressed in terms of liquid weight in order to overcome some limitations of the original optical method. Particularly the visual observation of the liquid front is not always clear and the observed level at the wall may not reflect the internal level since liquid rising can be non-homogeneous in the whole powder bed section, moreover the measurements can be affected by the subjectivity introduced by operator observation.

The weight w of the penetrated liquid is given by Eq. (9):

$$w = \varepsilon \rho \pi r_{eff}^2 h \quad (9)$$

After modification, combining Eqs. (5) with (6) and (9) Washburn's equation in terms of liquid weight can be derived:

$$\frac{w^2}{t} = C_w \frac{\rho^2 \gamma_{LV} \cos \theta}{\eta}, \quad (10)$$

where C_w is a geometric constant which accounts for the properties of particles arrangement in the packed bed. The determination of such constant is essential for a precise and accurate application of Washburn's equation. Unfortunately eq. 10 contains two unknowns, C_w and θ and cannot be solved uniquely. A first possibility to overcome this problem is the use of a completely wetting liquid (so that $\theta = 0$ and $\cos \theta = 1$). This allows to eliminate one unknown from eq. 10 and from the measured curve slope $\Delta w^2 / \Delta t$ the value of C_w can be determined provided the other liquid properties (η , γ_{LV} , ρ) are known. In this procedure repeatability and accuracy of sample preparation [24] as well as the

choice of the reference liquid are crucial steps [6]. Most of the reported studies in the literature focus on the choice of a completely wetting liquid for powders and the mainly used reference liquids are alkanes such as hexane, ciclohexane, heptane and octane [2, 23-26]. An alternative possibility is the direct estimation of C_w through air permeability measurements using the Kozeny-Carman model to describe the packing structure of the powder bed [24]

3. Experimental

3.1 Materials

Several mineral and metallic powders were selected in order to cover a range of material properties and collect information on wettability as a function of different bulk density (or bed porosity), particle size and chemical nature. Powders used in this experimental work are the raw materials used in the production of welding wires and they were supplied by Fileur®, Cittadella, Italy.

Particle size distributions were measured by sieving; the true density of the particles was determined by liquid pycnometry. Poured density was measured following the standard procedure ISO 3923/1 (International Organization for standardization, 1976). The procedure ISO 3953 was followed for measuring tap density: it requires vertically tapping a graduated container until the powder bed stabilizes at a minimum volume. These measurements were performed in triplicate and the average result is given in Table 1. Fe^a and Fe^b powders are both iron ores but they differ in terms of particle size distribution. All powders used in this work have not undergone any preparation or surface cleaning and were used 'as received'.

Table 1 Summary of the main physical powder properties.

Powder properties	d_{32} [μm]	True particle density [g/cm^3]	Poured density [g/cm^3]	Tap density [g/cm^3]
Fe ^a	42.24	7.684	2.483	2.840
Mn	14.08	6.969	2.887	3.558
Fe–Mn (C < 1%)	65.12	6.917	3.212	3.696
Fe–Mn (C < 8%)	86.24	9.742	3.106	3.509
Fe–Si	110.88	5.122	2.963	3.057
Fe ^b	129.36	7.812	2.884	3.003
TiO ₂	95.04	4.063	2.324	2.549

Potassium and sodium silicate is specifically recommended as a binder in the wet granulation process for the manufacture of consumable electrodes. Both of them are available in aqueous solutions. Potassium (K_2SiO_3) and Sodium Silicate (Na_2SiO_3) solutions are prepared by dissolving Potassium Silicate glass and Sodium Silicate glass in hot water respectively. By varying the silica to Potassium/Sodium Oxide (K_2O/Na_2O) ratio, products of definite but widely different properties are produced. Aqueous solutions of these polymeric binders at different concentrations in terms of water are selected to provide a range of viscosities, surface tensions and densities. Liquid viscosity was determined using a Haake RV3 rheometer, surface tension was measured using a KRUSS K6 tensiometer. The viscosity of these binders spanned a range of two orders of magnitude. Table 2 presents the physico-chemical properties of binder solutions.

Table 2 Physico-chemical properties of binder solutions at 20° C.

Binder liquid	Density ρ_L [g/mL]	Surface tension γ_{LV} [mN/m]	Viscosity η [Pa·s]
85.7 wt.% sodium silicate	1.303	59.2	0.031
50 wt.% sodium silicate	1.159	62.2	0.009
28.6 wt.% sodium silicate	1.086	65.3	0.006
85.7 wt.% potassium silicate	1.315	61.3	0.029
50 wt.% potassium silicate	1.163	63.3	0.007
28.6 wt.% potassium silicate	1.090	66.3	0.005

3.2 Sessile drop experiments

The experimental apparatus for sessile drop method consisted of a Petri dish containing about 80 g of powder corresponding to a layer 20 mm deep. A powder bed was formed by forcing the powder through a 150 μm sieve into the Petri dish and scraping the level with a metal spatula to make the powder surface smooth. A 5 μL micro syringe was positioned 20 mm above the bed surface and sessile drop penetration was filmed by Photron Fastcam-Pci video recorder operating at different frame rate: from 25 to 1000 frames/s. The drop sizes varied by 0.05 – 0.15 μL .

In order to investigate the wetting behaviour, the apparent contact angle θ was measured by drawing a tangent to the drop profile at the point of three-phase contact using the image analysis open-source software ImageJ (for general information see [27]). Other parameters which were measured included the radius of the drop before and immediately after the impact on the compact and the maximum radius reached during the spreading process. Three replicates were performed only for

the less dilute binder solutions. Figure 2 shows the sessile drop spread wetting for a metallic powder.

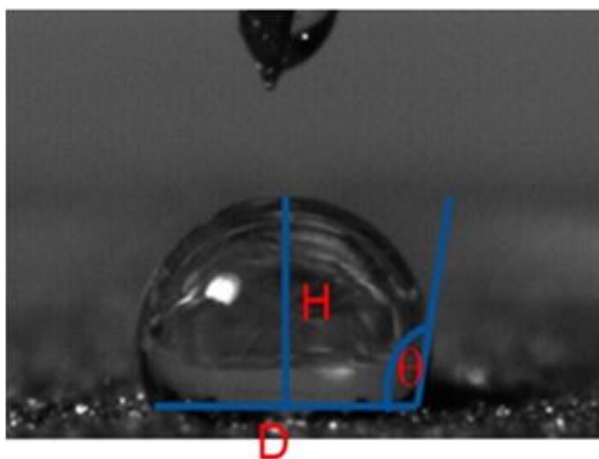


Fig. 2. Photograph of a potassium silicate droplet on Fe-Mn surface using the Photron Fastcam-Pci video recorder. The apparent contact angle θ , the diameter, D and the height, H of the droplet after the impact on powder are visualized.

3.3 Drop penetration time

The same experimental apparatus and procedure described in Section 3.2 were used to measure the drop penetration time which was defined as the time taken by the drop to penetrate completely into the powder bed.

Moreover for each powder the fluid rate penetration was determined as the ratio between the initial height of droplet and the drop penetration time. Results are reported in Table 3.

Table 3 Drop penetration results.

Powder	Binder fluid	Penetration time, t_p [s]	Penetration rate v_p [$\mu\text{m/s}$]	Contact angle, Θ [$^\circ$]
Fe ^a	85.7 wt.% sodium silicate	0.42 ± 0.02	3741.97 ± 517.27	87.50 ± 0.77
	85.7 wt.% potassium silicate	0.49 ± 0.09	3606.30 ± 225.26	83.00 ± 1.13
Mn	85.7 wt.% sodium silicate	3.95 ± 0.11	598.81 ± 74.82	89.50 ± 4.64
	85.7 wt.% potassium silicate	0.75 ± 0.16	2088.24 ± 434.15	74.75 ± 1.27
Fe-Mn	85.7 wt.% sodium silicate	0.79 ± 0.05	3097.00 ± 78.88	86.50 ± 2.12

Powder	Binder fluid	Penetration time, t_p [s]	Penetration rate v_p [$\mu\text{m/s}$]	Contact angle, Θ [$^\circ$]
(C < 1%)	85.7 wt.% potassium silicate	0.35 ± 0.10	6638.13 ± 673.38	83.30 ± 3.89
Fe-Mn	85.7 wt.% sodium silicate	0.65 ± 0.15	3905.08 ± 722.81	83.00 ± 1.41
(C < 8%)	85.7 wt.% potassium silicate	0.53 ± 0.03	3036.20 ± 298.16	78.85 ± 0.63
	85.7 wt.% sodium silicate	0.86 ± 0.02	1171.02 ± 264.28	87.58 ± 4.80
Fe-Si	85.7 wt.% potassium silicate	1.08 ± 0.09	2553.63 ± 222.64	89.80 ± 2.40
	85.7 wt.% sodium silicate	0.31 ± 0.01	7112.66 ± 123.51	85.15 ± 1.62
Fe ^b	85.7 wt.% potassium silicate	0.36 ± 0.03	7323.77 ± 17.91	80.70 ± 2.89
	85.7 wt.% sodium silicate	0.96 ± 0.05	2464.46 ± 402.28	85.92 ± 3.39
TiO ₂	85.7 wt.% potassium silicate	0.58 ± 0.13	3241.18 ± 138.97	69.80 ± 1.76

3.4 Washburn's experiments (weight based)

The experimental setup for weight measurement consisted of an aluminium cylindrical tube of 10 mm inner diameter and 60 mm height which had a nylon membrane placed at the bottom to sustain powder sample. A fixed quantity of powder has been weighted and placed in the capillary with a standard procedure that requires to fill the tube by pouring powder through a 150 μm sieve. The tube was connected to an electronic balance and weight data versus time were recorded with a frequency of 2 Hz as the imbibition proceeded. The data acquisition started when tube entered in contact with the probing liquid. Three replicates were performed for each system powder-binder. The experimental set up for capillary rise measurements and a typical output from Washburn method are provided respectively in Fig. 3 and Fig. 4.

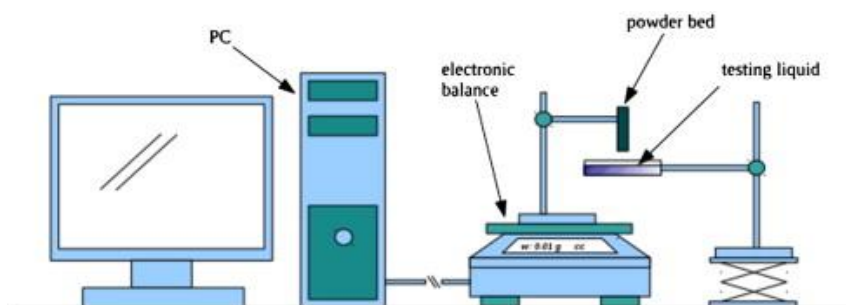


Fig. 3. Schematic diagram of experimental set up for Washburn's method.

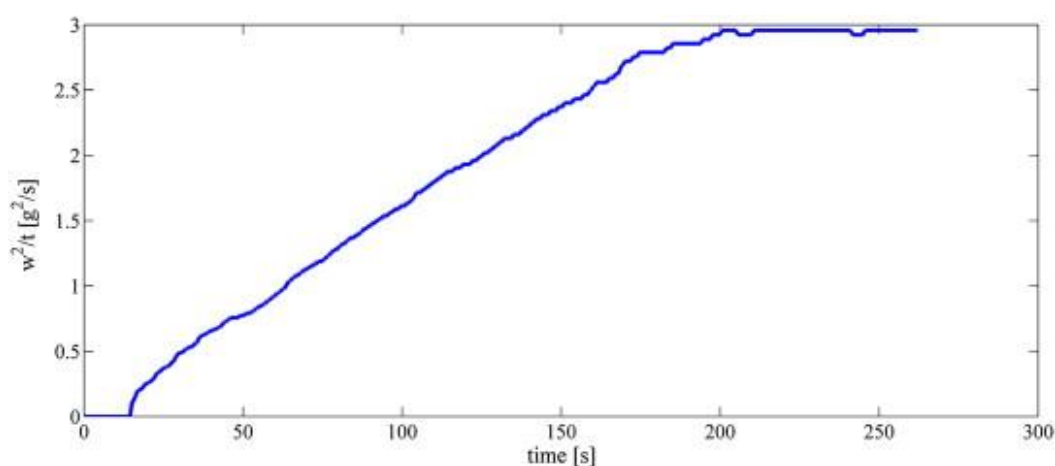


Fig. 4. Squared of weight gained by iron powder, w^2 , versus penetration time of potassium silicate.

Particular attention was paid in pouring the powders into the tube and in handling the tube after filling in order to have a strict powder packing control and get reproducible results. The results from all the experiments are discussed below.

4. Results and discussion

4.1 Sessile drop experiments

Figures from 5 to 7 illustrate a series of images taken with the high speed video camera of typical drop penetration experiments for potassium silicate-water solution on iron ore Fe^a, manganese and Fe – Mn (C < 1%) powders respectively. After the impact on the powder surface the liquid drop spread out and stretched quickly on the surface. At the same time it was drawn into the powder bed. The same behaviour has been observed for all the powders employed in the experiments. The infiltration of the fluids into the powders can be described as a balance of thermodynamic and kinetic contributions. The thermodynamic definition of contact angle according to Young-Duprè implies a force balance which allows to reach a final equilibrium shape of the droplet only if the

liquid drawing kinetics into the powder is low enough. So it is generally difficult to obtain contact angle measurements un-biased by the kinetic contributions.

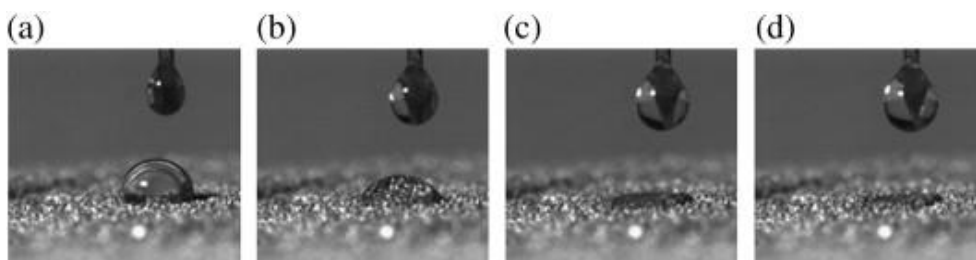


Fig. 5. Penetration of 85.7 wt% potassium silicate solution on iron. The picture are taken at (a) after the impact on powder compact, (b) 0.02 s, (c) 0.10 s, (b) 0.20 s and (d) 0.30 s after the impact.

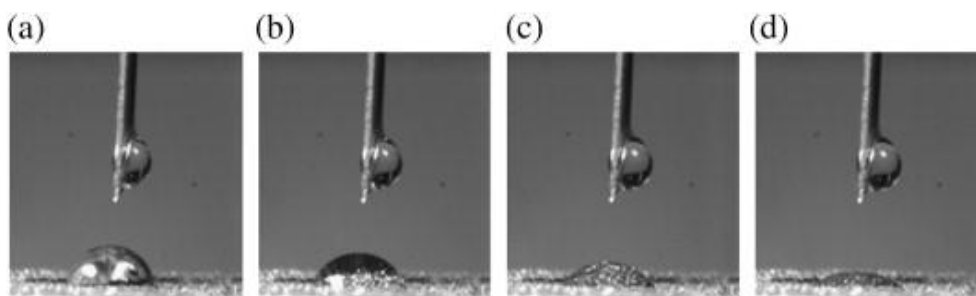


Fig. 6. Penetration of a 85.7 wt% potassium silicate drop on Mn powder. The picture are taken at (a) after the impact on powder compact, (b) 0.20 s, (c) 0.70 s and (d) 0.65 after the impact.

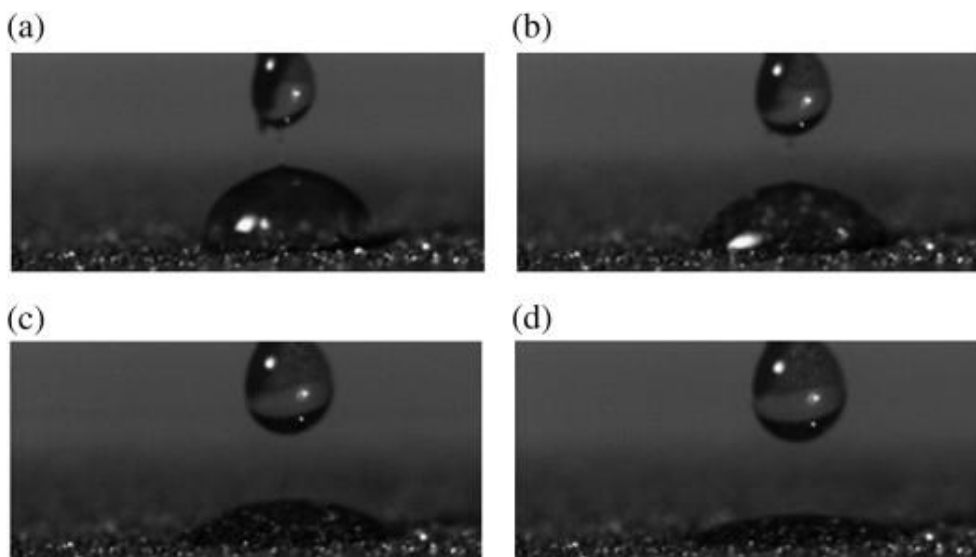


Fig. 7. Penetration of a 85.7 wt% potassium silicate drop on Fe - Mn powder. The picture are taken at (a) after the impact on powder compact, (b) 0.15 s, (c) 0.30s and (d) 0.45 after the impact. Table 3 shows the experimental mean drop penetration time and the standard error of the mean for each powder varying liquid binder. Table 3 also provides the fluid rate penetration and the contact

angle for the two different binders. The mean penetration rate is a more representative wettability index than the penetration time since it does not depend on the volume of the droplet. Because of the rough and irregular surface of the powders the measurements of the apparent contact angle by image analysis was not straightforward (see Figures 5 ÷ 7). It has been very difficult to identify the solid/liquid interface since the surface was not uniform. Therefore data are affected by operator error and they present relatively large standard errors as can be seen from Table 3. Nonetheless some general evidence can be collected.

All of the apparent contact angles measured are high and fall between 70 and 90 degrees. For the same powder the apparent contact angles are always greater for the sodium silicate excepted for the Fe–Si powder. Even if sodium and potassium silicate have similar physical properties fluid rate penetration can vary widely: from a minimum of 598.81 $\mu\text{m/s}$ for sodium silicate on manganese powder to 7112.66 $\mu\text{m/s}$ for the same binder on iron powder (Fe^b). We can observe that the same powder interacts differently with the binder: for example for manganese powder the fluid rate penetration can triplicate by varying the type of binder.

Moreover there is not a general trend between the fluid rate penetration and the contact angle values for the powder–liquid systems examined. Only for a subset of materials, iron (Fe^b), manganese, Fe–Mn ($C < 1\%$) and rutile powders, results where as expected, i.e. the larger the penetration velocity, the lower the contact angle.

4.2 Washburn experiments results

Table 4 summarizes Washburn's results for all the combination of powders and liquids used to investigate the wettability behaviour. It is interesting to note that liquid viscosity plays an important role: for the various binder solution the ranking of w^2/t matches with that of viscosity. The value of w^2 versus time vary by one order of magnitude with viscosity for the same kind of binder. For instance the more diluted potassium silicate solution has a slope w^2/t value of $17.5 \cdot 10^{-8} \text{ kg}^2/\text{s}$ on iron Fe^a powder while for the most concentrated solution the value is reduced by 90%. The same trend is shown for the sodium silicate.

Table 4 Values of the slope w^2/t [$10^{-8} \text{ kg}^2/\text{s}$] obtained from capillary rise experiments.

Powder	Binder fluid	Binder composition	w^2/t [$10^{-8} \text{ kg}^2/\text{s}$]
Fe^a	Potassium silicate	85.7 wt.%	1.650 ± 0.001
		50 wt.%	13.420 ± 0.012
	Sodium silicate	28.6 wt.%	17.500 ± 0.006
		85.7 wt.%	1.270 ± 0.002
		50 wt.%	10.350 ± 0.003
		28.6 wt.%	17.100 ± 0.011

Powder	Binder fluid	Binder composition	w^2/t [10^{-8} kg ² /s]
Mn	Potassium silicate	85.7 wt.%	0.380 ± 0.001
		50 wt.%	2.770 ± 0.002
		28.6 wt.%	3.810 ± 0.005
	Sodium silicate	85.7 wt.%	0.300 ± 0.001
		50 wt.%	2.610 ± 0.002
		28.6 wt.%	4.020 ± 0.004
Fe-Mn (C < 1%)	Potassium silicate	85.7 wt.%	0.670 ± 0.001
		50 wt.%	3.590 ± 0.002
		28.6 wt.%	6.810 ± 0.007
	Sodium silicate	85.7 wt.%	0.450 ± 0.001
		50 wt.%	3.780 ± 0.001
		28.6 wt.%	5.840 ± 0.005
Fe-Mn (C < 8%)	Potassium silicate	85.7 wt.%	0.320 ± 0.001
		50 wt.%	3.540 ± 0.002
		28.6 wt.%	4.480 ± 0.008
	Sodium silicate	85.7 wt.%	0.400 ± 0.001
		50 wt.%	2.640 ± 0.004
		28.6 wt.%	4.660 ± 0.007
Fe-Si	Potassium silicate	85.7 wt.%	0.400 ± 0.001
		50 wt.%	3.320 ± 0.012
	Sodium silicate	28.6 wt.%	5.220 ± 0.007
		85.7 wt.%	0.360 ± 0.002

Powder	Binder fluid	Binder composition	w^2/t [10^{-8} kg ² /s]
Fe ^b		50 wt.%	3.330 ± 0.003
		28.6 wt.%	4.060 ± 0.010
		85.7 wt.%	4.220 ± 0.006
	Potassium silicate	50 wt.%	23.760 ± 0.024
		28.6 wt.%	34.690 ± 0.082
		85.7 wt.%	2.420 ± 0.001
	Sodium silicate	50 wt.%	20.910 ± 0.023
		28.6 wt.%	34.600 ± 0.020
		85.7 wt.%	0.560 ± 0.001
TiO ₂	Potassium silicate	50 wt.%	6.140 ± 0.007
		28.6 wt.%	10.590 ± 0.001
	Sodium silicate	50 wt.%	5.730 ± 0.002
		28.6 wt.%	9.800 ± 0.008

Differently from the results of sessile drop experiments, Washburn data exhibited a clear trend with respect to the powder- liquid binder systems: all the powders showed more affinity (i.e. higher slope of the curve) for the potassium silicate solutions, independently of the dilution of the liquid binder. To determine the apparent contact angle between the liquid binders and the powders, the calculation of the constant term C_w is required. However, as mentioned in the Introduction, finding a total wetting liquid can be an issue for this kind of analysis. It has been indeed very difficult to find a total wetting liquid for our mineral and metallic powders, also because of a lack of information on this aspect in the literature. Therefore a dedicated study, addressed to the investigation of the best wetting liquid, has been carried out.

The first reference liquid used in the calibration method was n-heptane which is largely employed as total wetting liquid in literature [2, 21, 23, 25]. This preliminary step was carried out to assess the wettability of our most concentrated potassium and sodium silicates solutions since highly concentrated solutions are used in the wet granulation process for manufacturing of welding rods.

The values of constant C_W and $\cos\theta$ determined in this way are reported in Table 5. Three replicates were performed for each powder-liquid binder system.

Table 5 Washburn's results assuming n-heptane as total wetting liquid.

Powder	w^2/t (10^{-8} kg ² /s)	C [m ⁵]	87.5 wt.% potassium silicate		87.5 wt.% sodium silicate	
			$\cos\theta$ [-]	θ [°]	$\cos\theta$ [-]	θ [°]
Fe ^a	7.890 ± 0.007	3.21E-15	> 1	–	> 1	–
Mn	1.980 ± 0.001	8.07E-16	> 1	–	0.89	27.12
Fe–Mn (C < 1%)	2.910 ± 0.002	1.18E-15	> 1	–	> 1	–
Fe–Mn (C < 8%)	3.600 ± 0.001	1.52E-15	0.76	40.53	0.82	34.91
Fe–Si	3.40 ± 0.006	1.38E-15	0.79	37.81	0.67	47.93
Fe ^b	11.970 ± 0.007	4.87E-15	> 1	–	> 1	–
TiO ₂	4.510 ± 0.006	1.83E-15	0.83	33.90	0.62	51.68

Unfortunately we can see in Table 5 that for most of the powders the value of $\cos\theta$ exceeds unity meaning that the tested liquid wets the powder bed better than the reference liquids. Using an apolar reference liquid it is therefore possible to determine the contact angle only for few powders. Particularly n-heptane works well for Fe–Mn (C < 8%), Fe–Si and rutile powders.

For the choice of an appropriate liquid, hopefully working for all the powders of this study, it can be useful to characterize powders in terms of affinity to apolar and polar liquid. Yang and Chang [28] did an extensive study on the wettability of filter media using capillary tests. The wastewater treatment filters used were anthracite, manganese ore and quartz with size fraction in the range of 0.9–1.2 mm. The lipophilic to hydrophilic ratio (*LHR*) was employed to compare the selectivity of filter media towards oil and water in terms of wettability.

In the present work the *LHR* index was used to compare the difference of selectivity, in terms of wettability, between apolar and polar liquid for a specific powder. *LHR* was defined as:

$$LHR = \frac{\cos\theta_A}{\cos\theta_P}, \quad (11)$$

where θ_A and θ_P are respectively the apparent contact angle of an apolar liquid and a polar liquid with a powder. Combining Eqs. (10) with (11) this index can be written in terms of Washburn's equation variables:

$$LHR = \frac{(w_2/t)_A \eta_A \rho_P^2 \gamma_P}{(w_2/t)_P \eta_P \rho_A^2 \gamma_A} \quad (12)$$

For measuring the *LHR* value, apolar n-heptane and polar water, corresponding to the oil phase and the water phase in [29], were used in Washburn's experiments. Their properties are presented in Table 6.

Table 6 Properties of reference liquids at 20° C.

Reference liquid	Density ρ_L [g/mL]	Surface tension γ_{LV} [mN/m]	Viscosity η [mPa·s]
n-heptane	0.684	21.00	0.400
Water	1.000	72.10	1.002
Surfactant solution (a)	1.000	17.20	1.002
Surfactant solution (b)	1.000	21.50	1.002
Surfactant solution (c)	1.000	22.15	1.002

The slope of the lines w^2 versus time for the apolar and polar phases as well as the calculated *LHR* values are collected in Table 7.

Table 7 Wetting parameters and *LHR* values for all the powders.

Powder	n-heptane w^2/t [10^{-8} kg ² /s]	Water w^2/t [10^{-8} kg ² /s]	<i>LHR</i> [-]	Powder characteristic
Fe ^a	7.89	28.55	0.80	Hydrophilic
Mn	1.98	5.50	1.05	Lipophilic
Fe–Mn (C < 1%)	2.91	6.14	1.38	Lipophilic
Fe–Mn (C < 8%)	3.60	6.12	1.72	Lipophilic
Fe–Si	3.40	8.53	1.16	Lipophilic
Fe ^b	11.97	49.14	0.71	Hydrophilic
TiO ₂	4.51	15.27	0.86	Hydrophilic

Among the powders used, *LHR* values for iron powders are lower than one meaning that both of them are hydrophilic. The other powders have a *LHR* values larger than one so that they show a lipophilic behaviour. Manganese powder doesn't show a clear behaviour.

An apolar fluid like n-heptane was expected to be the best reference liquid for powders which exhibit a lipophilic behavior. Comparison with data from Table 5 however shows that for Fe–Mn (*C* < 1%) and Mn powders it is not possible to calculate the apparent contact angle by assuming n-heptane as total wetting liquid. It is also interesting to note that for rutile powder we can calculate the apparent contact angle even if rutile shows more affinity to polar fluids (*LHR* < 1).

At this point it can be interesting to perform a test on the same set of powders using water as total wetting liquid instead of n-heptane in order to verify how *LHR* behave with respect to the powders previously identified as hydrophilic in Table 7. Results are presented in Table 8.

Table 8 Washburn's results assuming water as total wetting liquid.

Powder	w^2/t [10^{-8} kg ² /s]	<i>C</i> [m ⁵]	87.5 wt.% potassium silicate		87.5 wt.% sodium silicate	
			$\cos\theta$ [-]	θ [°]	$\cos\theta$ [-]	θ [°]
Fe ^a	0.286 ± 0.007	3.91E-15	> 1	–	0.97	14.07
Mn	0.055 ± 0.003	7.53E-16	> 1	–	0.96	16.26
Fe–Mn (<i>C</i> < 1%)	0.061 ± 0.005	8.41E-16	> 1	–	> 1	–
Fe–Mn (<i>C</i> < 8%)	0.061 ± 0.001	5.11E-16	> 1	–	> 1	–
Fe–Si	0.085 ± 0.025	1.17E-15	0.94	19.94	0.79	37.81
Fe ^b	0.491 ± 0.053	6.73E-15	> 1	–	> 1	–
TiO ₂	0.153 ± 0.025	2.02E-15	0.75	41.40	0.56	55.94

Assuming water as the reference fluid, it is possible to determine a value of contact angle for the two iron powders and the sodium silicate (but not the potassium silicate). Some values of contact angle are obtained for manganese powder and Fe–Si powder but they are different (lower) than those obtained using n–heptane. This is due to the fact that these powders having a lipophilic behaviour exhibit an higher affinity to apolar liquid. On the contrary, the contact angle calculated for rutile and water are larger because of the hydrophilic behavior of this powder.

All these results suggest that the *LHR* can give only limited information on the affinity of the wetting medium with the powder and cannot be used as a general guide for the selection of the proper wetting fluid. They also confirm that Washburn's method is extremely sensitive to the choice

of the reference liquid used. For instance the rutile–potassium silicate system has an apparent contact angle ranging from 33° to 41° by changing the total wetting liquid.

4.3 Towards a total wetting liquid for metallic and mineral powders

Notwithstanding the difficulties in finding a total wetting liquid a further effort was made using surfactant aqueous solutions. It is known that partially or fully fluorinated hydrocarbon compounds exhibit outstanding chemical and thermal stability, low solubility in water and excellent lubricating properties because of their very low interfacial energy [30]. In fluorinated surfactants hydrogen atoms of the surfactant hydrocarbon tail are substituted by fluorine atoms to produce amphiphilic molecules with a fluorinated hydrophobic tail. Because of their low affinity with the aqueous solution fluorinated molecules exhibit a strong tendency to migrate to interfaces or surfaces and to orientate so that the polar hydrophilic group lies in water and the apolar hydrophobic group is placed out of it. This produce a superficial (air–aqueous solution) tension down to ~15 mN/m, which is twice as low as the value obtained with the best tension reducing hydrocarbon surfactants. Also interfacial tension (between condensed phases, i.e. particle surface–aqueous solution) is strongly lowered as a consequence of this migration. So three wetting media were prepared using different fluorinated compounds. Surfactant solution (a) was prepared by slowly dissolving 1 g of N-diethyl-3 heptadecafluoro-2 hydroxypropane-1 ammonium iodide in 999 g of cold water. Surfactant solution (b) had a concentration of 0.5 g/l of 1-perfluorotooctyl-3 propan-2 ol and finally surfactant solution (c) contained 0.5 g/l of N-benzyl-N,N-propyl-3 heptadecafluoro-2 hydroxypropane-1 ammonium bromide. These three solutions were expected to have the same physical properties of water in terms of density and viscosity because of their high dilution. Surface tension was the only physical property markedly different from that of water. Their characteristics are reported in Table 6.

A preliminary study was conducted for iron and Fe–Mn powders. These two powders have been chosen because their opposite behaviour in terms of LHR value. In Figure 8, Washburn's experiments for iron Fe^a powder were plotted. These three curves describe the wetting behaviour of the different surfactant solutions.

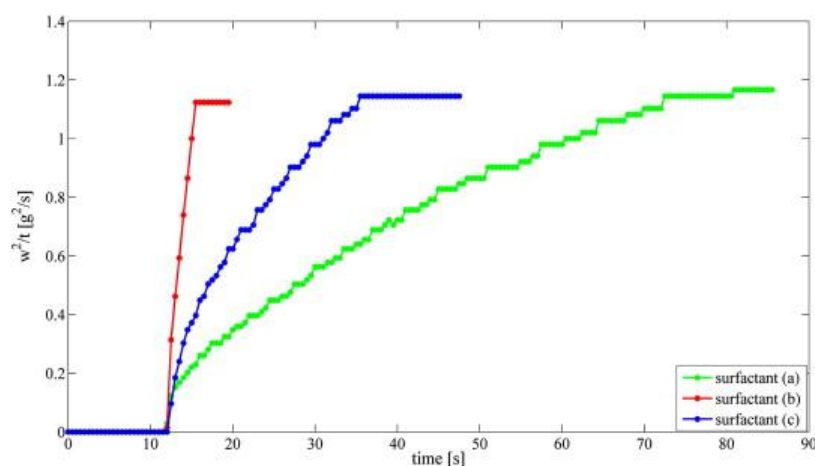


Fig. 8. The slope w_2 versus time for three different surfactant solutions on iron powder.

The curves presented in Figure 8 summarize the wettability behavior of the three surfactant solutions on iron powders. It can be observed that the rate of imbibition is clearly higher for the surfactant solution (b). The other powder exhibited the same behavior as summarized in Table 9.

Table 9 Washburn's results assuming surfactant solutions as total wetting liquids.

Powder	Surfactant (a) w^2/t (10^{-8} kg²/s)	Surfactant (b) w^2/t (10^{-8} kg²/s)	Surfactant (c) w^2/t (10^{-8} kg²/s)
Fe ^a	0.98	25.19	8.70
Fe ^b	1.68	29.07	1.49
Fe–Mn (C < 1%)	1.23	3.97	1.96
Fe–Mn (C < 8%)	1.61	5.22	3.60

Table 9 demonstrates that for the same powder the slope w^2 versus time is at least one order of magnitude larger in the case of surfactant (b). In particular it can be observed that sterical phenomena can play an important role on effectiveness of the wetting action. Surfactant in solution (b) presents indeed shorter and more rigid polar heads with respect to surfactants in solutions (a) and (c) which contain 'cumbersome' quaternary salts forming a tetrasubstituted polar head. This result in a more ordered, rod-like configuration of surfactant molecules (b) at the interface between particles surface and aqueous solution which determine a more effective lowering of the interfacial tension and can explain the observed increased wettability. For these reasons, the 1-perfluorooctyl-3 propan-2 ol solution can be considered as the best wetting liquid for the powders tested. The measured slopes for the fluorinated surfactant (b) leads to the constants C_w given in Table 10.

Table 10 Washburn's results assuming surfactant solutions (b) as total wetting liquids and relative values of contact angles for 87.5% wt potassium and 87.5% wt sodium solutions.

Powder	w^2/t (10^{-8} kg ² /s)	C_w [m ⁵]	87.5 wt.% potassium silicate 87.5 wt.% sodium silicate			
			$\cos\theta$ [-]	θ [°]	$\cos\theta$ [-]	θ [°]
Fe ^a	25.19 ± 0.01	1.17E-14	0.385	67.35	0.325	71.03
Mn	5.25 ± 0.01	2.44E-15	0.424	64.91	0.296	72.78
Fe–Mn (C < 1%)	3.97 ± 0.01	2.02E-15	0.901	25.71	0.614	52.12
Fe–Mn (C < 8%)	5.13 ± 0.01	2.39E-15	0.484	61.05	0.981	11.19
Fe–Si	7.08 ± 0.01	3.73E-15	0.334	70.49	0.249	75.58
Fe ^b	29.07 ± 0.07	1.64E-14	0.702	45.41	0.452	63.13
TiO ₂	11.08 ± 0.01	5.15E-15	0.296	72.78	0.220	77.29

The values of the constant C_w determined using surfactant solution (b), allowed us to determine the contact angles for all the tested powders according to Eq. (10). This means that the fluorinated solution (b) can be considered among the wetting liquid tested here the best total wetting liquid for the mineral and metallic powders examined.

4.4 Further comparisons

As final remark a comparison between capillary rise technique (Washburn) and sessile drop method is reported. In Table 11 the apparent contact angles obtained using the two methods are compared. It can be observed that it does not exist a clear correlation between the contact angles measured by the two different approaches. The apparent contact angles measured by sessile drop technique are larger than those calculated using Washburn's method but at a first sight it is difficult to identify which of the two methods provide with the most meaningful and realistic contact angle values. However if we consider the uncertainties introduced by the sessile drop measurement and summarized in the Section 3 (difficult assessment of droplet equilibrium after the impact on powder compact and of droplet position because of contemporary sinking in the compact, difficult assessment of a perfectly flat surface for the compact, collapse of the compact because of the droplet weight and capillary forces), the capillary rise method should be expected to perform better. This hypothesis is confirmed by plotting data of Table 11 separately.

Table 11 Comparison between the contact angles calculated by sessile drop and Washburn's method.

Powder	87.5 wt.% potassium silicate		87.5 wt.% sodium silicate	
	Sessile drop method	Washburn's method	Sessile drop method	Washburn's method
	θ [°]	θ [°]	θ [°]	θ [°]
Fe ^a	83.00	67.35	87.5	71.00
Mn	74.75	64.91	89.50	72.80
Fe–Mn (C < 1%)	83.30	25.71	86.50	52.13
Fe–Mn (C < 8%)	78.85	61.06	83.00	58.45
Fe–Si	89.80	70.49	87.58	75.58
Fe ^b	80.70	45.41	85.15	63.09
TiO ₂	69.80	72.78	85.92	77.29

Figure 9 and Figure 10 compare the apparent contact angle values estimated by the sessile drop method and Washburn technique respectively. The binders compared in each Figure are the two liquid binders of industrial relevance, i.e the solutions at 87.5% in weight of potassium and sodium silicate in water. Sodium and potassium silicate are both used industrially because they have very similar physical properties (see Table 2). We can observe that in the case of the sessile drop method there is not a simple correlation between experimental data for the same powder. Washburn method instead exhibits a clear correlation between the apparent contact angle values reflecting the similarity of the two liquid binders. Moreover Washburn technique spans over a larger range of angles for both binders. This finding suggests also that Washburn method has a higher sensitivity than the sessile drop one.

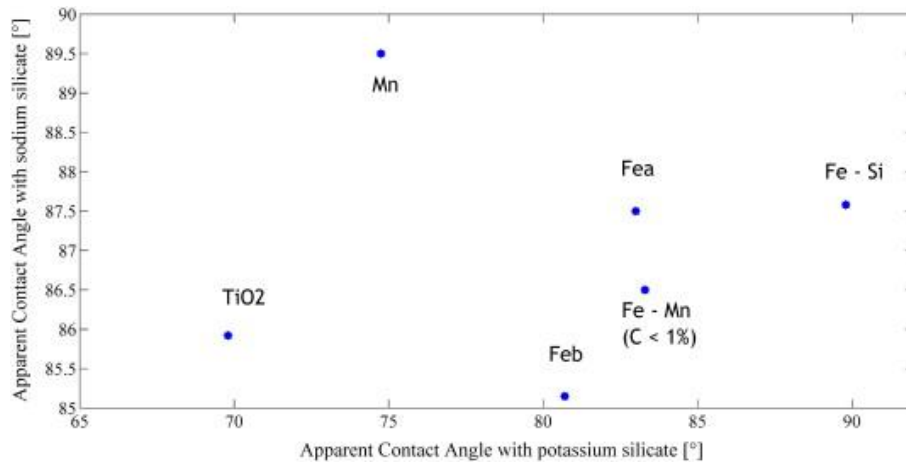


Fig. 9. Comparison of the apparent contact angles values using sessile drop method for the two binder liquids of industrial relevance.

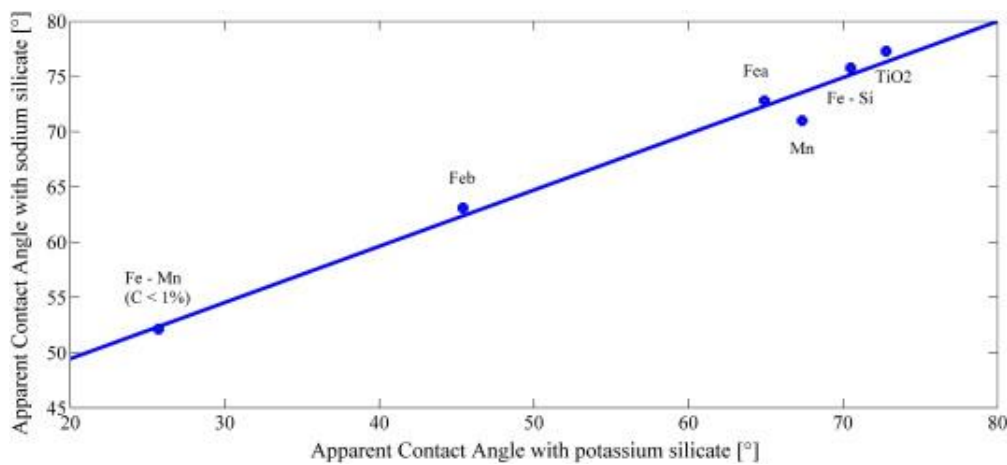


Fig. 10. Comparison of the apparent contact angles values using Washburn method for the two binder liquids of industrial relevance.

5. Conclusions

Investigation of wettability of mineral and metallic powders using the sessile drop technique and Washburn test was carried out. The objective was to collect information on wetting behavior of powders which are widely used in the powder metallurgy, particularly in the manufacture of welding rods.

For the drop penetration experiments, this work confirms that the drop penetration behaviour is quite complex and highly dependent on the structure of powder bed. For non-ideal surfaces such as mineral and metallic powder, kinetics plays a more important role than thermodynamics in dictating

wettability. Variables linked to kinetics, such as binder viscosity, seem to have the major role. For this reason fluid rate penetration is a more significant wetting index than the apparent contact angle in the sessile drop approach. The main weakness in the sessile drop method is that it is very difficult to get reproducible data as the results are very sensitive to how the powder compacts are prepared. Moreover it is not easy to recognize the correct instant when the drop penetration starts and this aspect can also affect the measurements of penetration time and rate.

Concerning Washburn's experiments, it is important to note that the choice of the best wetting liquid is a critical step because it affects the calculation of the material constant C_w and then the measurements of the apparent contact angle. This work showed that for the mineral and metallic powders tested the reference liquids so far most commonly used in the literature (alkanes) are not suitable. The data demonstrate that a surfactant solution containing fluorinated ethers was the most appropriate total wetting liquid because it wetted better than the test liquid and the value of $\cos \theta$ never exceeded unity for all the powders tested. On the whole Washburn's method performed much better than sessile drop method for the several powders tested in this work. The use of fluorinated liquids was a practical solution for the powder tested however in general there is not an universal reference liquid for all the possible powders and the determination of the constant C_w remains a major limitation of this approach. As a future work it is therefore advisable to develop methods such as that used by [24] or [26] which does not require a calibration step with a total wetting liquid and improve our ability to evaluate C_w on the base of basic physical properties of the powder packed bed (porosity, tortuosity, particle shape and size distribution).

Acknowledgements

The author wishes to acknowledge Prof. L. Conte and his research group at the Department of Industrial Engineering, University of Padova (Italy) for supplying the fluorinated surfactants. The authors also thank Fileur® – Trafilerie di Cittadella Spa (Cittadella, Italy) for supplying the powder formulations and liquid binders and for providing a financial support of this work.

References

- [1] W. Pietsch, Size enlargement by agglomeration. Wiley, Aarau; Salle and Sauerländer, Chichester, 1991.
- [2] J. Litster and B.J. Ennis, The science and engineering of granulation process, Kluwer academic publishers, Dordrecht, The Netherlands, 2004.
- [3] D.M. Parikh, Handbook of pharmaceutical granulation technology, 2nd ed., Taylor and Francis Informa Publications, 2005 191–228.
- [4] J.D. Litster, B.J. Ennis, S.M. Iveson, K.P. Hapgood, Nucleation, growth and breakage phenomena in agitated wet granulation processes: a review. *Powder Technology* 117 (2001) 3-39.
- [5] M. Lazgab, S. Khashayar, I. Pezron, P. Guigon and L. Komunyer, Wettability assessment of finely divided solids. *Powder Technology* 157 (2005) 79-91.
- [6] T.T. Chau, A review of techniques for measurement of contact angle and their applicability on mineral surfaces. *Mineral Engineering* 22 (2009) 213-219.
- [7] P.G. de Gennes, Wetting: static and dynamics. *Review of Modern Physics* 57 (1985) 827-863.

- [8] K.P. Hapgood and B. Khanmohammadi, Granulation of hydrophobic powders. *Powder Technology* 189 (2009) 253-262.
- [9] A. Marmur, Equilibrium contact angles: theory and measurement. *Colloids and Surface A: Physicochemical and engineering Aspects* 116 (1995) 55-61.
- [10] N.W.F. Kossen and P.M. Heertjes, The determination of the contact angle for systems with a powder. *Chemical Engineering Science* 20 (1967) 593-599.
- [11] D.W. Fuerstenau, J. Diao, J. and M.C. Williams, Characterization of the wettability of solids particles by film flotation 1. Experimental investigation. *Colloids and Surface* 60 (1991) 127-144.
- [12] E.W. Washburn, The dynamic of capillary flow. *Physical Review* 17 (1921) 273.
- [13] M. Lago and M. Araujo, Capillary rise in porous media. *Physica A: Statistical Mechanics in porous media* 289 (2001) 1-17.
- [14] J.C. Feeley, P. York, B.S. Sumbly and H. Dicks, Determination of surface properties and flow characteristic of salbutamol sulphate, before and after micronisation. *International Journal of Pharmaceutics* 172 (1998) 89-96.
- [15] I. Krycer, I., D.J. Pope and J.A. Hersey, An evaluation of tablet binding agents part I. Solution binders. *Powder Technology* 34 (1983) 39-51.
- [16] B. Waldie, Growth mechanism and the dependence of granule size on drop size in fluidized-bed granulation. *Chemical Engineering Science* 46 (1991) 2781-2785.
- [17] S.H. Shaafsma, P. Vonk and N.W.F. Kossen, Proc. World Congress on Particle on Particle Technology 3, Brighton, UK, July 6-9, 1998, IChemE.
- [18] K.P. Hapgood, J.D. Litster, S.R. Biggs and T. Howes, Drop Penetration into Porous Powder Beds. *Journal of Colloid and Interface Science* 253 (2002) 353-366.
- [19] D. Zhang, J.H. Flory, S. Panmai, U. Batra and M.J. Kaufman, Wettability of pharmaceutical solids: its measurement and influence on wet granulation. *Colloids and Surfaces A: Physicochemical and Engineering Aspects* 206 (2002) 547-554.
- [20] A. Siebold, A. Walliser, M. Nardin, M. Oppliger and J. Schultz, Capillary Rise for Thermodynamic Characterization of Solid Particle Surface. *Journal of Colloid and Interface Science* 186 (1997) 60-70.
- [21] A. Siebold, M. Nardin, A. Walliser, J. Schultz and M. Oppliger, Effect of dynamic contact angle on capillary rise phenomena. *Colloid and Surface in A: Physicochemical and Engineering Aspects* 161 (2000) 81-87.
- [22] L. Labajos-Broncano, M.L. Gonzales-Martin, J.M. Bruque, C.M. Gonzalez-Garcia and B. Janwzuk, On the Use of Washburn's Equation in the Analysis of Weight-Time Measurements Obtained from Imbibition Experiments. *Journal of Colloid and Interface Science* 219 (1999) 275-281.
- [23] S.M. Iveson, H. Susana and S. Biggs. Contact angle measurements of iron powders. *Journal of Colloid and Surface A: Physicochemical and Engineering Aspects* 166 (2000) 203-214.
- [24] L. Galet, S. Patry. Determination of the wettability of powders by the Washburn capillary rise method with bed preparation by a centrifugal packing technique. *Journal of Colloid and Interface Science* 346 (2011) 470-475.
- [25] B.J. Ennis, Theory of granulation: an engineering perspective. In: Parikh, D.M. (Ed.), *Handbook of Pharmaceutical Granulation Technology*, 2nd ed. Taylor and Francis Group, New York, 2006.

Susana, L., Campaci, F., Santomaso, A.C. Wettability of mineral and metallic powders: Applicability and limitations of sessile drop method and Washburn's technique (2012) *Powder Technology*, 226, 68-77. (DOI: [10.1016/j.powtec.2012.04.016](https://doi.org/10.1016/j.powtec.2012.04.016))

[26] G.K. Tampy, W. Chen, M.E. Prudich and R.L. Savage, Wettability Measurements of Coal Using a Modified Washburn Technique. *Energy & Fuels* 2 (1988) 782-786.

[27] M.D. Abramoff, P.J. Magalhaes and R.J. Ram, Image Processing with ImageJ. *Biophotonics International* 11 (2004) 36-42.

[28] R.K. Holman, M.J. Cima, S.A. Uhland, S.A. and E. Sachs, Spreading and infiltration of inkjet-printed polymer solutions droplets on a porous substrate. *Journal of Colloid and Interface Science* 249 (2002) 432-440.

[29] B.W. Yang and Q. Chang, Wettability studies of filter media using capillary rise test. *Separation purification technology* 60 (2007) 335-340.

[30] A. Zaggia, L. Conte, G. Padoan and F. Ceretta, Synthesis and characterization of partially of fluorinated ethers. *Journal of Fluorine Chemistry* 131 (2010) 844-851.